Edith Cowan University

Research Online

ECU Publications Pre. 2011

2009

Opto-VLSI-Based Broadband True-Time Delay Generation for Phased Array Beamforming

Budi Juswardy
Edith Cowan University

Feng Xiao
Edith Cowan University

Kamal Alameh
Edith Cowan University

Follow this and additional works at: https://ro.ecu.edu.au/ecuworks

 Part of the Engineering Commons

This is an Author's Accepted Manuscript of: Juswardy, B. , Xiao, F. , & Alameh, K. (2009). Opto-VLSI-Based Broadband True-Time Delay Generation for Phased Array Beamforming. Proceedings of POEM 2009. (pp. 7516-43). Wuhan, China. SPIE, USA. Available here

Copyright 2009 Society of Photo-Optical Instrumentation Engineers (SPIE). One print or electronic copy may be made for personal use only. Systematic reproduction and distribution, duplication of any material in this paper for a fee or for commercial purposes, or modification of the content of the paper are prohibited.

This Conference Proceeding is posted at Research Online.
https://ro.ecu.edu.au/ecuworks/590

Opto-VLSI-based broadband true-time delay generation for phased array beamforming

Budi Juswardy*, Feng Xiao, and Kamal Alameh

Western Australia Center for MicroPhotonic Systems, Edith Cowan University
270 Joondalup Drive, Joondalup WA6027, AUSTRALIA;

ABSTRACT

Electronically controlled phased-array antennas can adaptively scan radiated beams in three-dimensional space without mechanically moving parts. While most of the research on phased-array antennas has been focusing on broadband beam steering less attention has been devoted to null steering. Broadband null steering requires a beamformer that can generate variable and frequency independent true time-delays (TTD). In this paper we propose and demonstrate the concept of an Opto-VLSI-based tunable true-time delay generation unit for adaptive null steering in phased array antennas, where arbitrary single or multiple true-time delays can simultaneously be synthesized. Simulated azimuth gain patterns for a 4-element antenna arrays is presented, and experimental results are shown, which demonstrate the principle of the proposed true-time delay unit.

Keywords: Phased-array antenna; Fourier optics; Optical signal processing; Microwave photonics; True-time delay generation.

1. INTRODUCTION

The processing of Radio Frequency (RF) and microwave signals using optics for antenna array system is more advantageous as compared to fully electronic circuits or Digital Signal Processor (DSP) typically used to control the antenna array beamforming. Optical signal processing offers attractive features such as small size, low weight, immunity to electromagnetic interference (EMI) and, especially, the capability to generate true-time delay (TTD) for broadband beamforming in phased-array antenna, with minimal beam squint.

Most of the research on optical phased-array antenna has been focused on broadband beam steering and less attention has been given to null steering, which is the ability to maintain nulls at chosen angular coordinates for a broad frequency range [1]. Broadband null steering requires a beamformer that can generate variable and frequency independent true-time delays (TTD). This variable TTD requirement is difficult to achieve using conventional electronic phase-shifter circuits or DSP.

In this paper, we propose and demonstrate the principle of a true-time delay unit capable of generating variable and frequency independent TTD. The proposed true-time-delay unit also has the capability to generate multiple true-time delays for several antenna elements simultaneously, making it attractive for broadband null-steering in phased array antennas.

2. SYSTEM DESCRIPTION

Our proposed TTD generation unit employs an Opto-VLSI processor, a broadband optical source using Amplified Spontaneous Emission (ASE), and high dispersion fibers that can be reconfigured to synthesize multiple arbitrary time delays. The following sections describe the principle of beam steering and the architecture of a phased array antenna that employs Opto-VLSI processor for TTD generation needed for broadband null steering.

2.1 Principle of broadband null steering

The typical array factor (or directional response) of an N-element phased-array antenna architecture is given by [1]:

* Author contact information:
E-mail: b.juswardy@ecu.edu.au Telephone: +61 8 6304 5146

$$AF_N(\theta) = \prod_{n=1}^{N-1}(x - x_n) = \sum_{m=0}^{N-1} W_m x^m \quad (1)$$

where $x = \exp[jkd\sin(\theta)]$, d is the antenna element spacing, k = wave number = ω/c, and $x_n = x$ (θ_n) is a zero of the polynomial AF_N corresponding to an antenna null at the angular coordinate θ_n. Note that a change of even one zero affects all the weights, W_m. Note also that with N antenna elements, the phased-array antenna can synthesize only (N–1) nulls, as evident from Equation (1).

Generally, for an N-element broadband phased array, the synthesis of (N–1) broadband nulls can be achieved if the beamformer of the antenna can adaptively generate and combine (2^{N-1} –1) delayed versions of the RF signals received by the antenna elements [2] as illustrated in Fig. 1.

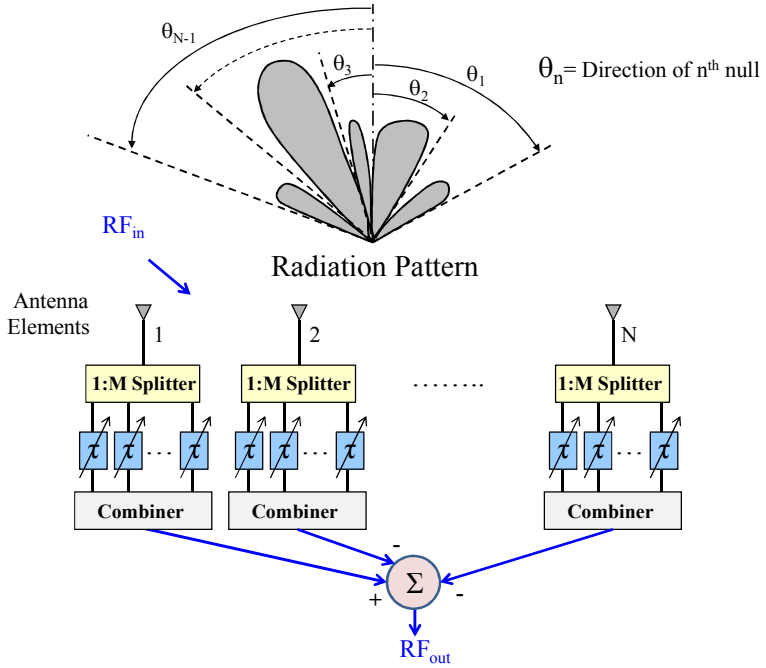

Figure 1. Phased array antenna architecture for broadband null steering [2].

2.2 Principle of Beam Steering using Opto-VLSI

An Opto-VLSI processor is an array of liquid crystal (LC) cells controlled by a Very-Large-Scale-Integrated (VLSI) circuit on the bottom side of the LC [3], as shown in Fig 2(a). Digital holographic diffraction gratings could be applied to the processor, which makes it capable of steering/shaping incident optical beams, as illustrated in Fig. 2(b). The voltage level of every pixel can individually be controlled by applying a discrete voltage level on each pixel through the aluminium mirror electrode, across the LC cell. A transparent Indium-Tin Oxide (ITO) layer is used as the second electrode, and a quarter-wave-plate (QWP) layer is deposited between the LC and the aluminum mirror to accomplish polarization-insensitive operation [4].

By driving the Opto-VLSI processor with different blazed gratings pitches, optical beam steering can be achieved as shown in Fig. 2(b). The diffraction (or steering) angle for an Opto-VLSI processor, α_m, is given by [2]:

$$\alpha_m = \arcsin\left(\frac{m\lambda}{d}\right) \quad (2)$$

where m is the diffraction order (usually only the first order is considered), λ is the light wavelength in vacuum, and d is the grating period. By addressing each pixel independently a phase hologram can be synthesized leading to optical beam steering, beam shaping or multicasting. This steered optical beam can be employed to generate TTD for RF signal, as will be explained in the next section.

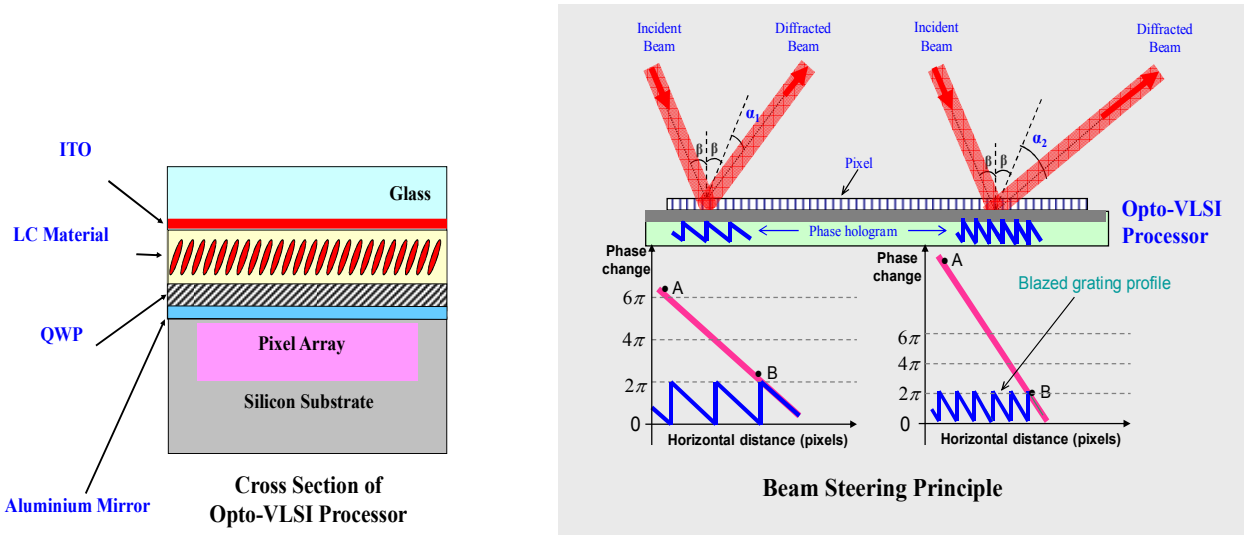

Figure 2. (a) Opto-VLSI processor cross sectional view. (b) Principle of beam steering through variable-pitch blazed grating generation.

2.3 Architecture for broadband null steering

Figure 3 shows the proposed Opto-VLSI-based RF phased array antenna architecture for broadband null steering. A wideband amplified spontaneous emission (ASE) source is used as an optical source, and it is split into N parts where N is the number of antenna elements. The RF signal received by each antenna modulates the ASE source that is routed to the Electro-Optic Modulator (EOM) connected to each antenna element. Each RF-modulated optical signal is then routed into an Erbium Doped Fiber Amplifier (EDFA) for amplification, and then collimated and launched into a diffractive grating plate. The latter demultiplexes the collimated ASE signal into wavebands (of different center wavelengths) along different directions and maps them onto the surface of a 2-D Opto-VLSI processor that is partitioned into N rectangular pixel blocks. Each pixel block is assigned to an antenna element and used to generate the delays required for that antenna element. Each pixel block is further partitioned into *M* rectangular sub-pixel-blocks, where each sub-pixel-block is assigned to an RF-modulated waveband. By driving a sub-pixel-block with an appropriate phase hologram the RF-modulated waveband can be steered either along the incident path thus being coupled into its corresponding fiber collimator for maximum weight synthesis or off-track for arbitrary weight generation.

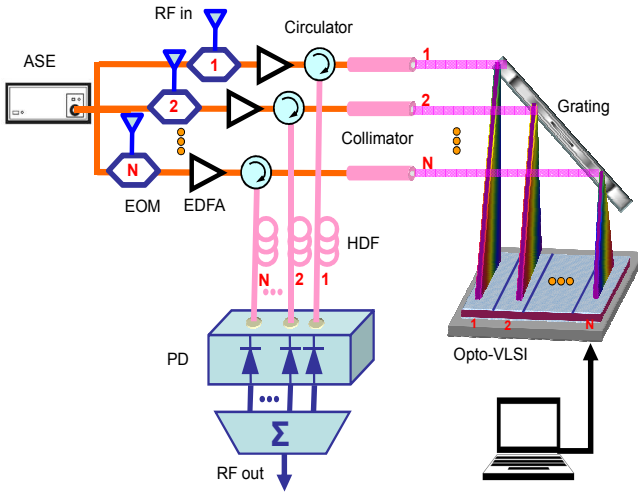

Figure 3. Opto-VLSI-based phased array antenna architecture for broadband null steering.

Single or multiple arbitrary RF-modulated wavebands can be coupled back into the fiber collimators and the amplitude of each selected waveband can also be controlled simply by uploading the appropriate phase holograms that drive the various pixel-blocks of the Opto-VLSI processor.

The RF-modulated wavebands coupled into the fiber collimators are then routed via optical circulators to high dispersion optical fibers (HDFs), where they experienced true-time delays that depend on their centre wavelengths. The delayed RF-modulated wavebands in the HDFs are finally detected by a photo-receiver array, and combined with appropriate polarities to synthesize the required nulls.

One of the attractive features of the Opto-VLSI-based phased array antenna architecture shown in Fig. 3 is its ability to generate multiple RF delays without the need for RF splitters. Furthermore, the amplitude weight of each generated RF delay sample can simultaneously be controlled, which adds another dimension to synthesis beam and null steering. This architecture offers excellent flexibility in null steering because multiple true-time RF delays for each antenna element can simultaneously be synthesized using computer generated holograms.

Fig. 4 shows the simulated polar plot (a) and azimuth gain pattern (b) for a 4-element antenna array based on the structure depicted in Fig. 3. The spacing between the antenna elements is half the RF wavelength. The Minimum Mean-Square Error (MMSE) algorithm was used to generate null objectives at -60°, -20° and 45°, and desired beam directions at 10°.

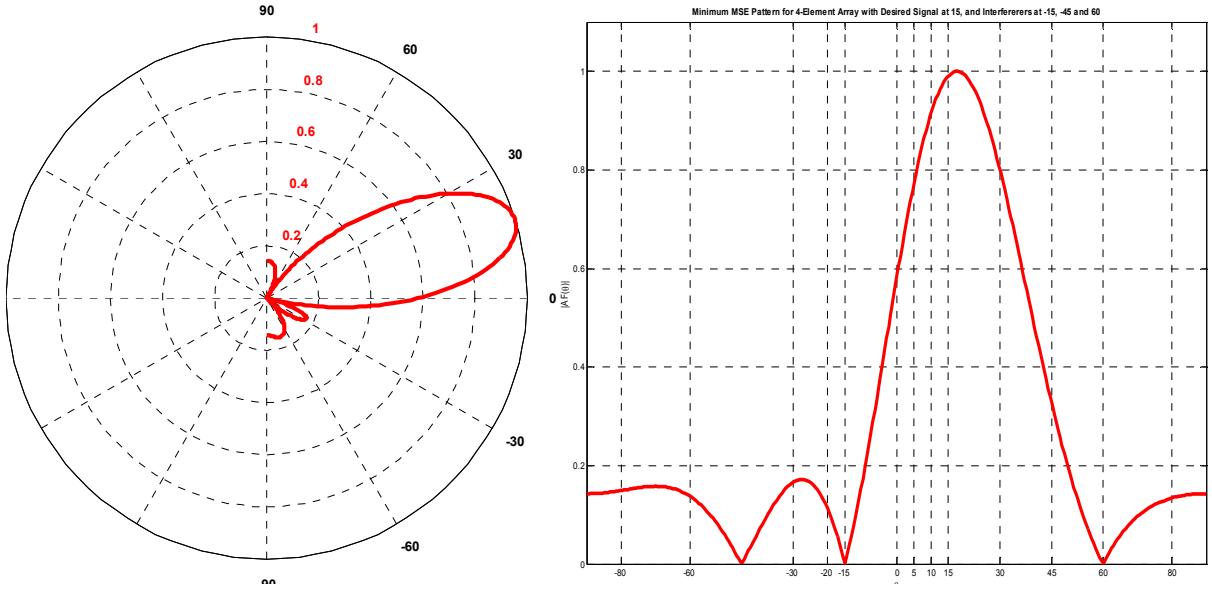

(a) (b)

Figure 4.Simulated polar plot (a) and azimuth gain pattern (b) of the proposed Opto-VLSI-based phased array antenna.

3. EXPERIMENTAL SETUP

To demonstrate the principle of the phased-array antenna architecture shown in Fig. 3, some experiments have been performed using the setup illustrated in Fig. 5. In this setup, a broadband ASE source was modulated, via a JDS Uniphase electro-optical modulator (EOM), by an RF signal which was generated using a 20 GHz network analyzer. The RF-modulated optical signal was amplified by an EDFA, collimated at 1-mm diameter and then launched onto a diffractive grating plate. The grating demultiplexed the ASE beam into multiple RF-modulated wavebands, which were then mapped onto the active window of a 1×4096-pixel Opto-VLSI processor with 256-phase-level, 1-μm pixel size and 0.8-μm dead spacing between adjacent pixels.

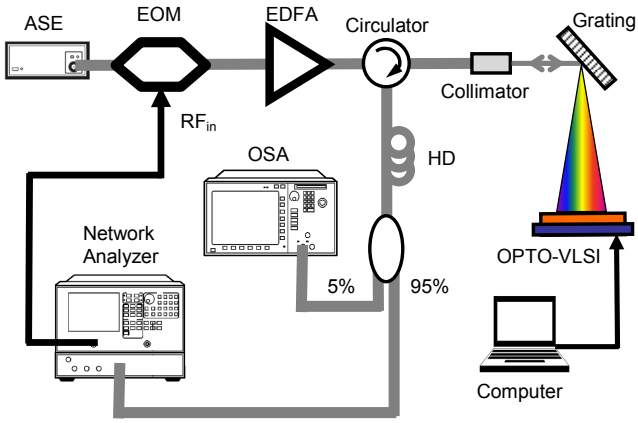

Figure 5. Experimental setup used to demonstrate tunable time delay generation

A computer program was developed to generate optimised phase holograms into the Opto-VLSI, so that it can steer the specific RF-modulated wavebands back into the fiber collimator, and at the same time capable of equalizing the waveband intensities by changing the maximum phase levels applied to the different pixel blocks [3].

Figure 6 illustrate how the optical waveband could be selected by using the principle of beamsteering using Opto-VLSI. Any number of beam could be steered back to simultaneously generate multiple time delays. For example, by applying an appropriate phase holograph consisting of 5 sections of different blazed gratings, 5 different wavebands could be steered back and coupled to the collimator, as shown in Fig. 6. By changing the size and the phase of the pixels, the selected wavebands can be tuned in terms of their wavelength separation and amplitude.

To generate the time delay, the selected wavebands were then routed via a circulator to a 22-km high dispersion fiber (HDF) with dispersion coefficient of 382.5 ps/nm and insertion loss of 4.6 dB. An optical spectrum analyzer (OSA) was used to monitor the 5% of spectrum as detected by a photoreceiver port built in the Network Analyzer, as illustrated in Fig. 5.

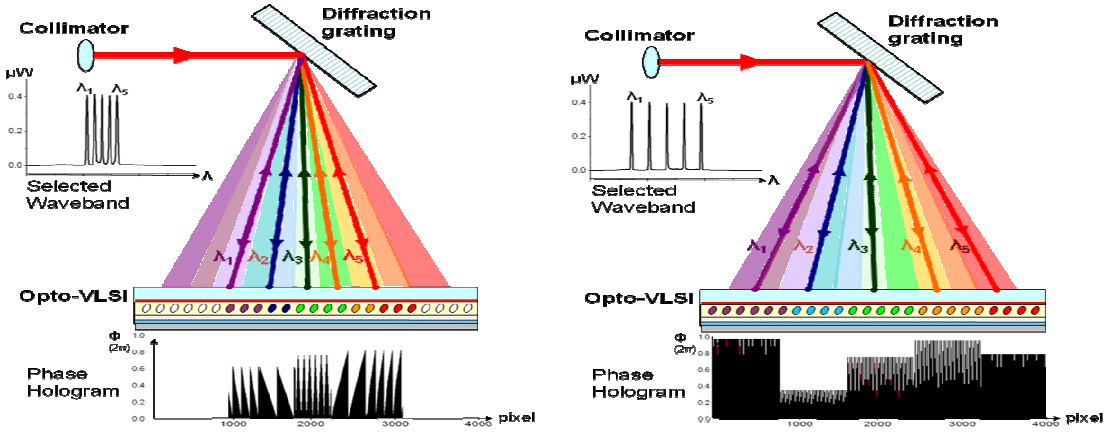

Figure 6. The principle of optical waveband selections.

The RF response produced after the photodetection of the delayed RF-modulated wavebands was monitored using network analyzer, where the true-time-delay between the wavebands could be deduced. The RF transfer function that results from detecting delayed optical wavebands can be described with the following equation [6]:

$$H(f) = \sum_{r=0}^{M} a_r \exp[-j2\pi r f \tau] \tag{3}$$

Where f is the RF frequency, M is the number of the detected RF-modulated wavebands, a_r is the r^{th} tap weight, which is proportional to the optical power of the r^{th} waveband, and τ is the time delay between adjacent wavebands introduced by the high dispersion fiber. The free spectral range of the transfer function is given by the following equation [5]:

$$f_{FSR} = \frac{1}{\tau} \tag{4}$$

The time delay, τ, can also be expressed in terms of the dispersion of the HDF as

$$\tau = \alpha \cdot \Delta\lambda \tag{5}$$

where α denotes the dispersion coefficient of the HDF, and $\Delta\lambda$ is the wavelength separation between the centers of two adjacent wavebands.

Note that the time delay, τ, depends on the dispersion coefficient of the dispersion medium as evident from Eq. 5. Therefore, a higher dispersion fiber optics results in a longer time delay generated.

Different phase holograms were applied to the Opto-VLSI processor to generate five equally-separated RF-modulated optical wavebands with wavelength separations between 1.74nm and 6.84nm as shown in Fig. 7. The network analyser monitors the RF responses of the photodetection of these five optical wavebands

Equation 4 is used to calculate the true time delay based on the measured free spectral ranges of the RF spectrums shown in Fig. 7. In addition, the measured optical waveband spacing was also used to calculate the time delays using Eq. 5 for a comparison. Table 1 summarizes the free spectral ranges of the various measured RF responses, the measured waveband separations, and their corresponding time delays based on the result depicted in Figure 7, calculated using Eq. 4 and Eq. 5. There is a good agreement between the true-time delays calculated using Eq. 4 and Eq. 5.

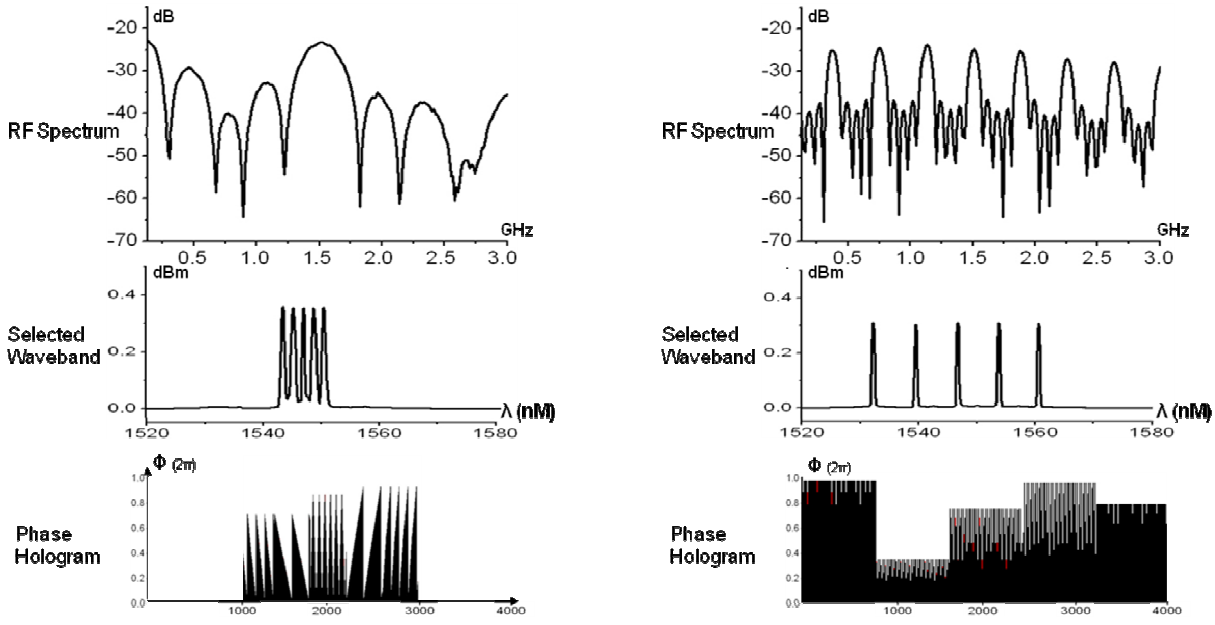

Figure 7: The measured RF spectrum responses (top figures) due to the photodetection of modulated optical wavebands (middle figures) and the phase hologram (bottom figures) that is used to generate 5 optical waveband with separation of 1.74nm (a) and 6.84nm (b) between each waveband.

Table. 1. Measured free spectral ranges, waveband separations, and their corresponding time delays (calculated using Eq. 4 and Eq. 5).

	Figure 7 (a)	**Figure 7 (b)**
Measured waveband separation (nm)	**1.74**	**6.84**
Measured FSR (GHz)	**1.51**	**0.39**
Time delay (ns) calculated using Eq.5	**0.67**	**2.63**
Time delay (ns) calculated using Eq.4	**0.66**	**2.58**

The RF insertion losses of the whole tunable true-time delay system, defined as the RF power ratio between input and output of the RF signal, can be approximately expressed as [7]:

$$T_{RF} = \frac{P_{RF\,out}}{P_{RF\,in}} = \left(\frac{\pi P_{opt} T_{opt} Z_0}{2V_\pi} R \right)^2 \tag{6}$$

Where Z_0 is the effective EOM RF input impedance or resistance of the EOM electrode, V_π is the voltage for a π-radian optical phase shift, R (A/W) is the photodetector responsivity, P_{opt} is the input continuous wave (CW) optical power to the EOM, and T_{opt} is the optical power transmission parameter that accounts for all the optical losses and/or gain in the optical processing including the EOM insertion losses.

In this experiment, the RF insertion loss is mainly due to the free-space optical system including the fibre collimator, the diffraction grating and the Opto-VLSI processor, which contributes around 12.5dB loss. The high dispersion fibre (HDF) and the EOM have insertion loss 4.6dB and 3.8dB, respectively. The total optical insertion loss of the entire system is around 21dB, whereas the EDFA provides a low gain of about 10dB due to saturation. The overall RF insertion loss in the experiment was about 25dB. This RF insertion loss can be compensated for by the use of an optical amplifier of 12.5dB gain placed after the HDF (before photodetection).

Finally, the experimental results shown in Fig. 7 and Table 1 confirm the ability of the Opto-VLSI-based true time delay unit to adaptively generate arbitrary RF delays for broadband null steering of phased array antennas. In order to generate multiple RF true-time delays for each antenna element, the Opto-VLSI processor was driven by optimised phase holograms that select and couple appropriate RF-modulated wavebands into a HDF that simultaneously delays the selected wavebands. To measure the generated time delays simultaneously, the selected wavebands were detected by a photodetector to generate a microwave transversal filter response whose FSR and shape factor (measured by the network analyzer) can be used to calculate the amplitudes and delay times of the wavebands.

4. CONCLUSION

We have proposed and demonstrated the principle of an Opto-VLSI-based tunable true-time (TTD) delay generation unit for adaptively steering the nulls of RF phased array antennas. In particular, the control of the time delay generation unit and FSR have experimentally been verified through the use of optimized computer-generated phase holograms uploaded onto an Opto-VLSI processor. The proposed TTD unit is capable of generating multiple arbitrary true-time delays of up to 2.5 ns.

REFERENCES

1. H. Zmuda, E. N. Toughlian, and P. M. Payson, “Broadband Nulling for Conformal Phased Array Antennas Using Photonic Processing,” IEEE International Topical Meeting on Microwave Photonics, MWP 2000, 17-19 (2000).
2. B. Juswardy, F. Xiao, and K. Alameh, "Opto-VLSI-based photonic true-time delay architecture for broadband adaptive nulling in phased array antennas," Opt. Express 17, 4773-4781 (2009).
3. F. Xiao, B. Juswardy, K. Alameh, and Y. T. Lee, “Novel broadband reconfigurable optical add-drop multiplexer employing custom fiber arrays and Opto-VLSI processors,” Opt. Express 16, 11703-11708 (2008).
4. I. G. Manolis, T. D. Wilkinson, M. M. Redmond, and W. A. Crossland, “Reconfigurable multilevel phase holograms for Optical switches,” IEEE Photon. Technol. Lett. 14, 801–803 (2002).
5. J. Capmany, B. Ortega, et al., “Discrete-time optical processing of microwave signals,” J. Lightw. Technol. 23, 702-723 (2005).
6. H. R. Rideout, J. S. Seregelyi, and J. Yao, “A True Time Delay Beamforming System Incorporating a Wavelength Tunable Optical Phase-Lock Loop,” J. Lightw. Technol. 25, 1961-1770 (2007).
7. J. Capmany, B. Ortega, and D. Pastor, “A tutorial on Microwave photonic filters,” J. Lightw. Technol. 24, 201-229 (2006).